

DYNAMIC ANALYSIS OF A DOUBLE IMPACT TRIAXIAL TEST ON SAND BY THE FINITE ELEMENT METHOD

Mohammed Y. Fattah⁽¹⁾

Omar al-Farouk S. al-Damluji⁽²⁾

Yousif J. al-Shakarchi⁽³⁾

(1) Assistant Professor, Building and Construction Engineering Department, University of Technology, Baghdad, Iraq, Email: myf_1968@yahoo.com.

(2) Former Professor, Civil Engineering Department, University of Baghdad, Iraq.

(3) Former Professor, Civil Engineering Department, University of Baghdad, Iraq.

ABSTRACT: Impact problems have recently been the subject of intense research. Impact tests have found a great interest by several researchers, and dynamic testing apparatus were developed in different laboratories. In addition, several theoretical models were developed to simulate impact tests theoretically and get the corresponding stress-strain relations.

A general mixed finite element formulation ($u - w - \pi$) is presented in this paper. This formulation includes the inertia effects and the materials (solid grains and water) are considered compressible. The application of this formulation in solving impact problems of dry sand is made by restricting the boundary conditions concerning the pore fluid, and comparisons are made between laboratory tests conducted at the University of Baghdad in 1989 against elasto-plastic model named ALTERNAT are made herein. A comparison is made between the experimental results and theoretical ones which are obtained by simulating the impact tests using the finite element method. The ALTERNAT model gave very good predictions for displacements of dense ($D_r = 75\%$) sands when subjected to double impacts.

Keywords: Double impact, triaxial test, finite elements, dynamic.

1. Introduction

Porous media, such as soil rock and other materials can be idealized as two -phase continua composed of a deformable solid skeleton and a fluid that saturates the pores in the skeleton. The determination of the transient response for such porous media is important in a number of engineering problems. One of the important problems is the impact one and the response of soils to falling masses. Impact problems have recently been the subject of intense research.

2. Governing Equations for Dynamic Problems:

The governing equations include dynamic relations, continuity and constitutive equations. A complete derivation of the dynamic equations is given by Biot (1962). In a given problem, the loading rate and permeability of the porous medium play a key role in determining the time scale and the method of solution to be used. When relatively rapid loads are applied and permeability is low, an undrained analysis is possible, i.e., the load rate is greater than the pore fluid diffusion rate. For situations with relatively slow loading and high permeability, i.e., where the load rate is less than the pore fluid diffusion rate, a drained analysis is possible. Soil dynamic problems lie between the undrained and drained extremes where dynamic loading is applied and transient pore fluid motion is significant, (Simon et al., 1986).

2.1 Effective Stress and Constitutive Relations

Pure statics allows us to divide the total stress state into two parts, one of these being the hydrostatic pressure, P , acting externally and internally on the pore fluid and the other is the effective stress (*principle of effective stress*), thus (Zienkiewicz and Bettess, 1982):

$$\sigma_{ij} = \sigma'_{ij} - \delta_{ij}P \quad (1)$$

where σ_{ij} is the total stress, σ'_{ij} is the effective stress and δ_{ij} is Kronecker's delta.

In soil mechanics, the slight deformations of volumetric nature caused by a pore pressure increase are generally neglected, but in less porous materials, these deformations can be computed as (Zienkiewicz and Taylor, 2000):

$$d\varepsilon_{ij} = \delta_{ij}dP/3K_s \quad (2)$$

where K_s is the average bulk modulus of the solid grains forming the skeleton.

Having postulated the virtually negligible effect of the pressure P on the total strain, ε_{ij} , one can imply that most of the deformations are due to the effective stresses or other extraneous causes such as for instance temperature. One can thus write (Lewis and Schrefler, 1998):

$$d\varepsilon_{ij} = d\varepsilon_{ij}^{\sigma} + d\varepsilon_{ij}^{\bar{}} + d\varepsilon_{ij}^0 \quad (3)$$

where: $d\varepsilon_{ij}^{\sigma}$ = strains due to stresses.

$d\varepsilon_{ij}^0$ = strains due to temperature, creep, etc, (autogeneous strains).

The rate-independent constitutive law relates $d\sigma_{ij}$ to $d\varepsilon_{ij}^{\sigma}$ by (Zienkiewicz and Taylor, 2000):

$$d\sigma'_{ij} = D_{ijkl} d\varepsilon^{\sigma}_{kl} \quad (4)$$

where D_{ijkl} describes the components of the elasticity tensor.

On the other hand, the plastic behaviour of soils can be accounted for by using a more general constitutive relation such as:

$$\sigma'_{ij} = D_{ijkl} (\varepsilon_{kl} - \varepsilon^p_{kl}) \quad (5)$$

where ε^p_{ij} is the permanent plastic strain tensor.

The permanent plastic strain is related to the residual pore pressure by (Zienkiewicz et al., 1982):

$$P = -\beta \varepsilon^o_v \quad (6)$$

where:

$$\beta = \frac{1}{\frac{1}{K_T} + \frac{n}{K_f}}$$

K_T = tangent bulk modulus of the skeleton,

K_f = bulk modulus of water,

n = porosity, and

ε^o_v = volumetric plastic strain = ε^p_{ii} .

2.2 Continuity Equation:

Biot (1962) started his analysis by considering the kinetic energy of a unit volume of a solid –fluid mixture in terms of the average displacement of the solid, u_i , and the average displacement of the fluid, U_i . Zienkiewicz and Bettess (1982) assumed that both the solid grains and water to be incompressible. Mei and Foda (1982) reasoned that the volume changes are due to the existence of air pockets entrapped in the pores. Their equation for a two - phase material in the Eulerian space is given as:

$$n \dot{U}_{i,i} + (1 - n) \dot{u}_{i,i} = -\frac{n}{\beta} \dot{P} \quad (7)$$

where: β = the effective bulk modulus of elasticity.

($\dot{\quad}$) represents differentiation with respect to time.

Awad (1990) applied a general form of the continuity equation considering the solid grains and fluids to be compressible, thus:

$$\dot{u}_{i,i} + \dot{w}_{i,i} + \frac{1}{K_b} \dot{P} + \frac{u_i}{K_b} P_{,i} + \frac{w_i}{K_w} P_{,i} = 0 \quad (8)$$

where: w_i is the displacement vector of the fluid with respect to solid, and

K_b is the bulk modulus of the soil-water sample.

$$\frac{1}{K_b} = \frac{n}{K_w} + \frac{1-n}{K_s} \tag{9}$$

K_s = the bulk modulus of the solids.
 K_w = the bulk modulus of water.

2.3 Boundary Conditions:

Two types of boundaries exist, the first one, S , surrounding the bulk, and the other, \bar{S} surrounding the fluid.

At each boundary, the stresses at any time, t , are known at a position and the displacement is known at the remaining portion. This can be written as follows:

$$u_i(x,t) = \hat{u}_i(x,t) \quad \text{on } S_1 \tag{10}$$

$$\tau_{ij}(x,t) n_j(x) = \tau_{i(x,t)} \quad \text{on } S_2 \tag{11}$$

$$W_i(x,t) n_j(x) = P(x,t) \quad \text{on } \bar{S}_1 \tag{12}$$

$$-P_i(x,t) n_j(x) = P(x,t) \quad \text{on } \bar{S}_2 \tag{13}$$

where n_i is a unit normal vector and the superscript (^) represents a known function.

By choosing the appropriate boundary conditions for \bar{S} , one can control the drainage conditions.

In this paper, the soil considered is dry, i.e., the terms concerning the pore fluid are neglected, and this was done by considering that the sample is fully drained through choosing appropriate boundary conditions.

3. Some Approximations to Dynamic Equations:

The use of the full solution in terms of the u/w variables represents six variables in three dimensions (or four in two dimensions). This formulation is called $(u-w)$ formulation, (Simon et al., 1986). In this paper, a more general formulation will be used which is called $(u-w-\pi)$ model where π is the model pore fluid pressure in the finite element discretization. In this model, both the solid grains and fluids are assumed to be compressible. The model also takes into account the fluid inertia effects.

It is rational to think that this model best represents the behaviour of granular materials under dynamic loading and especially the blast one due to the large voids in such materials. This is attributed to the shape, size and arrangement of particles which allow easy movement of the pore fluid and this, in turn, increases the fluid inertia. This formulation can be verified when high frequency loads are applied, (Zienkiewicz and Bettess, 1982).

4. The ALTERNAT Model:

The model described in this paper forms the major component of a double hardening model for the mechanical behaviour of sand under alternating loading. The model was developed by Molenkamp (1987) at Delft Geotechnics. In Figure (1), the yield surfaces of both plastic models, namely the “compressive” and the “deviatoric” models are shown in the stress space of the isotropic stress, s , and the deviatoric stress, t .

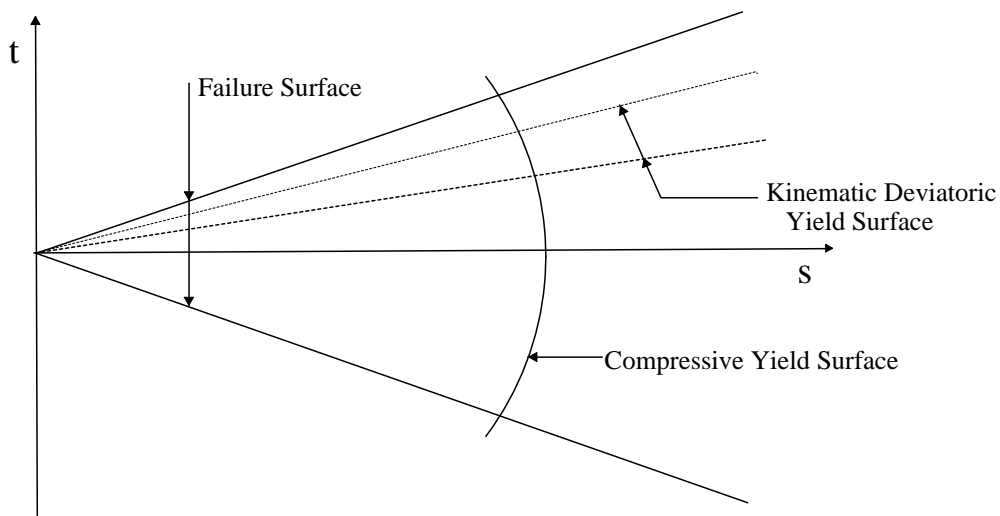


Fig. 1. The yield surfaces of the ALTERNAT model.

4.1 The Yield Surface for the Deviatoric Model:

For the continuum model of a uniform stack of rigid discs, a kind of kinematic yield surfaces was found (Figure 2) in which the relevant measure of stress appeared to be a shear stress level (Molenkamp, 1980). For the present kinematic model, a similar measure of a relevant stress is introduced, namely the shear stress level which is defined by:

$$\frac{t_{ij}}{\frac{I_1}{3}} = \frac{\sigma_{ij} - \frac{I_1}{3} \delta_{ij}}{\frac{I_1}{3}} \tag{14}$$

in which: t_{ij} = deviatoric stress.

$I_1 = \sigma_{ij} \delta_{ij}$ = first stress invariant.

This relevant measure of stress is dimensionless.

For the tensor of anisotropy, also a dimensionless deviatoric tensor, ξ , is introduced, thus $\xi_{ij} \xi_{ij} = 0$. The relevant measure of the pseudo shear stress level becomes:

$$\frac{X_{ij}}{\frac{I_1}{3}} = \frac{t_{ij}}{\frac{I_1}{3}} - \xi_{ij} \tag{15}$$

in which: X_{ij} = deviatoric pseudo stress tensor.

The expression chosen for the yield surface F^d should reduce to a generally accepted expression for monotonic loading when $\xi_{ij} = 0$. The expression as introduced by Lade and Duncan (1975) is used:

$$F^d = \frac{I_1^3}{I_3} - 27 - f^d(x) = 0 \tag{16}$$

in which:

$$f^d = \frac{I_1^3}{I_3} - 27 \text{ is a measure of the shear stress level, constant at a kinematic yield surface for a}$$

definite value of the hardening parameter, χ , as shown in Figure (2). I_3 is the third stress invariant.

4.2 The Plastic Potential for the Deviatoric Model:

In a plastic material model, the plastic potential describes the ratio of the Eulerian strain rates. For simplicity, it is assumed that the ratios of the plastic Eulerian strain rates can be described in the following way:

$$\dot{\xi}_{ij}^d = \dot{\lambda} \left\{ \alpha \xi_{ij} + \frac{\partial G^{dd}}{\partial \sigma_{ij}} \right\} = \dot{\lambda} \frac{\partial G^d}{\partial \sigma_{ij}} \tag{17}$$

in which:

$$\frac{\partial G^{dd}}{\partial \sigma_{ij}} \xi_{ij} = \mathbf{0} = \text{deviatoric tensor} \tag{18}$$

and
$$\frac{\partial G^{dd}}{\partial \sigma_{kl}} \frac{\partial G^{dd}}{\partial \sigma_{kl}} = 1 \tag{19}$$

α is the *angle of noncoaxiality* which is the angle between the principal directions of stress and the Eulerian strain rates.

Like the yield surface, the deviatoric component of the plastic potential G^{dd} is based on the failure surface of Lade and Duncan (1975), namely:

$$F^* = \frac{I_1^{3*}}{I_3^*} - 27 - f^{d*} = \mathbf{0} \tag{20}$$

in which: I_1^*, I_3^* are the first and third invariants of the pseudo stress T_{ij}^* . The pseudo stress T_{ij}^* has the same isotropic component as the pseudo stress $T_{ij} = \sigma_{ij} - I_1/3$ as used for the yield surface but a smaller deviatoric part.

Details of the above mentioned functions and the ALTERNAT model are given by Molenkamp (1987) and Fatah (1999).

4.3 Stress Dilatancy:

Molenkamp (1980) elaborated on the stress dilatancy theory for triaxial compression and triaxial extension tests. For loading towards failure in triaxial compression, it was found that:

$$\frac{\dot{V}}{\dot{\gamma}} = \frac{-\sqrt{2}(1-K) - (2+K)\frac{t}{s}}{(1+2K) + \sqrt{2}(1-K)\frac{t}{s}} \tag{21}$$

in which:

$$K = \tan^2\left(45 + \frac{\phi_o}{2}\right)$$

V = volumetric strain,

γ = deviatoric strain, and

φ_o = the interparticle friction angle.

It is assumed that (Molenkamp, 1980):

$$\phi_o = \phi_{cv} - (\phi_{cv} - \phi_{\mu}) \exp\left(\frac{-s}{Pa \cdot S_{cv}}\right)$$

in which:

φ_μ = interparticle friction angle at very low isotropic stress, s,

φ_{cv} = interparticle friction angle at very high isotropic stress,

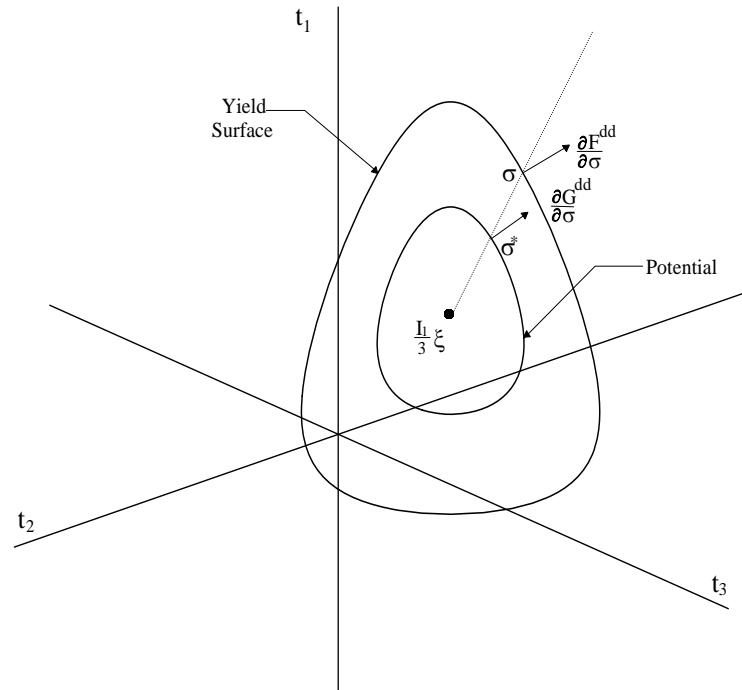
S_{cv} = parameter describing the rate by which φ_o changes from φ_μ to φ_{cv} with increasing isotropic stress level (s/Pa), (see Figure 3), and,

Pa = atmospheric pressure.

For loading towards failure in triaxial extension, it was found that:

$$\frac{\dot{V}}{\dot{\gamma}} = \frac{\sqrt{2}(1-K) - (1+2K)\frac{t}{s}}{(2+K) - \sqrt{2}(1-K)\frac{t}{s}} \tag{23}$$

Details of the functions and the ALTERNAT model are given by Molenkamp (1980) and Fatah (1999).



Note: t_1 , t_2 and t_3 are the principal stresses.
 Fig 2. The yield surface and the plastic potential.

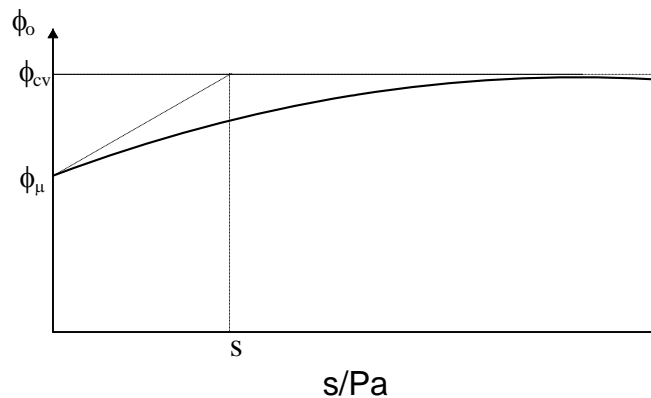


Fig. (3) – Definition of the parameters for stress dilatancy.

4.4 Extension of the ALTERNAT Model:

In the numerical simulation of the behaviour of frictional materials under alternating loading, the small errors in the calculation of each individual increment may accumulate partly in subsequent increments. This property of numerical models is known as "numerical drift". Molenkamp (1990) described an algorithm to minimize eventual numerical drift due to cyclic loading. One aspect involves the automatic control of the magnitude of the applied subincrements of stress and strain. The other aspect concerns a corrective procedure to keep the relevant stresses on the corresponding yield surfaces. Consequently, eventual errors in the plastic deformation will not accumulate. A combination of the parameters of the previous version of the ALTERNAT model (1987) and the present one will be used in this paper. The range of validity of the ALTERNAT model had been extended by Molenkamp (1990) from strain to large strain deformation. To this end, also the concept of the critical state had been applied. Details of the application are given by Fatah (1999).

4.5 Determination of the ALTERNAT Model Parameters:

For the determination of the parameters of the ALTERNAT model described in the previous sections, special types of triaxial tests are required, e.g., drained triaxial tests with monotonically increasing or decreasing axial strain and constant isotropic stress. These tests are not easy to be conducted in soil mechanics laboratories. It is

intended here to choose a simple theoretical model to get the required stress - strain relationships for the determination of ALTERNAT model parameters.

Of many theoretical models available to predict the overall response of sands, the endochronic model was chosen for this task. This model treats the sand as a non-linear elasticplastic material. Furthermore, the theory assumes inelastic changes to be caused only by the rearrangement of grains.

In this paper, the original version of the endochronic theory adopted by Bazant and Krizek (1976) is used because of its numerical simplicity. This version was limited to drained conditions and will be extended to include undrained conditions. Fattah (1999) gave a detailed investigation about using the endochronic model in determining ALTERNAT model parameters. For the description of the ALTERNAT model parameters, see Molenkamp (1987 and 1990).

5. The Computer Program:

The program (LIQUEFAC) was developed which is an extensive modification of the program (BLAST) developed by Awad (1990) at Colorado State University. The program was modified to take into account different types of dynamic loading such as blast, impact and earthquake loading. It was arranged into a modular form in order to minimize the run time.

Since the (u-w- π) formulation adopted in this paper results in an unsymmetric effective stiffness matrix, the subroutines ACTCOL and UACTCL (Zienkiewicz, 1977) are used instead of subroutine LDUSKY of the program (BLAST). These subroutines are utilized for symmetric and unsymmetric equation solving, respectively.

6. Testing Program:

6.1 Dynamic Testing Apparatus:

A special apparatus was designed and constructed from available components at the College of Engineering of the University of Baghdad by Namiq et al. (1990). The dynamic testing apparatus used in this investigation consists mainly of three parts as shown in Figure (4).

- A- The frame and the hammer.
- B- The modified triaxial cell.
- C- The electronic measuring system.

6.2 The Frame and the Hammer:

A four legged steel channel frame was constructed (Figure 5). This frame is 2.65 m high with a square base of 0.9 m by 0.9 m. Each two adjacent legs were braced together in order to give an overall rigidity to the frame, Figure (5). The frame supports centrally a vertical pipe with 82 mm internal diameter acting as a guide to the falling mass and the hammer. A slit was made along one side of the pipe. It serves as a monitor for the visual determination of the level of the hammer in the pipe. The mechanism for raising the hammer, or falling mass, consists of a system of jack, rollers, pulleys and a steel cable. An aluminum catch is attached to the cable inside the pipe and acts as a tool to catch and lift the hammer, (Farhan ,1989) .

The falling mass system was manufactured with the following characteristics (Baho, 1989):

1. The axis of fall of the mass is coincident with the axis of the ram of the cell.
2. Different weights and heights of the falling mass can be used.
3. The falling mass, after impact, travels a prescribed distance which can be changed as desired (see Figure 5).
4. The falling mass stops after hitting the ram to allow the sample to vibrate freely.

6.3 The Modified Triaxial Cell:

A 100 mm Standard Wykeham Farrance triaxial cell was modified for this purpose. The pedestal was removed and a new aluminum pedestal was especially manufactured to mount the load cell taking special precautions to pass the electric cable through the pedestal and without damage. The cell ram was replaced by an especially manufactured ram made from aluminum. The displacement transducer was added inside the cell. It was connected to the base of the cell to allow the confining fluid to enter the cell without restriction.

The soil specimen rests on the bottom load cell with a special aluminum cap which is firmly seated on the load cell probe. A special opening was made in the cap to allow for evacuating air from the sample by connecting the system to a vacuum pump through the modified pedestal (Farhan, 1989).

6.4 The Electronic Measuring System:

The axial deformations of the soil specimen were measured by a strain gauge, displacement transducer type TML CDP-25 with a range of movement equal to 25 mm and a gauge factor equal to 2.0.

The force at the bottom of the sample is measured by a load cell type TML CLP-500 KA. The force at the top of the sample is measured by a load cell type TML TCLP-500 KA.

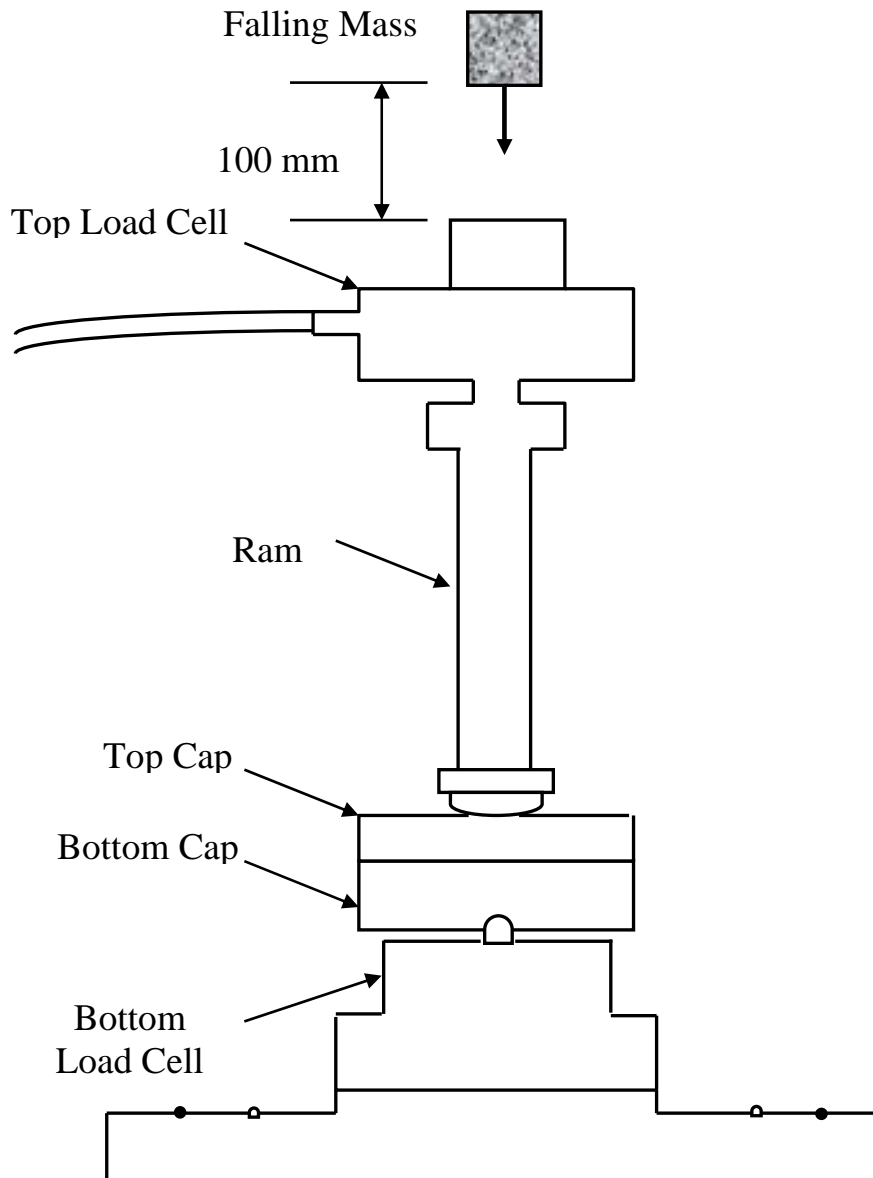


Fig. (4) - Arrangement of apparatus for dynamic testing.

6.5 The Soil Tested:

The soil tested was a uniform silica sand from Al-Ruttba region, western Iraq. The sand was washed and sieved on sieve No. 40 (0.42 mm) and was retained on sieve No. 50 (0.297 mm). Thus a uniform sand was obtained so that no segregation takes place during sample preparation.

The specific gravity, G_s , was measured to be 2.65. The sand tested had a uniformity coefficient, C_u , equal to 1.23, and a coefficient of concavity, C_c , equal to 0.93. The effective diameter of the sand was 0.38 mm. The minimum dry density, γ_{dmin} , was found to be equal to 1.376 gm/cm^3 and that produced a maximum void ratio equal to 0.93. The maximum dry density, γ_{dmax} was found to be equal 1.675 gm/cm^3 . The corresponding void ratio was equal to 0.58.

The diameter of the sample was chosen to be 76 mm, and the height 152 mm. This yields an L/D ratio of 2:1.

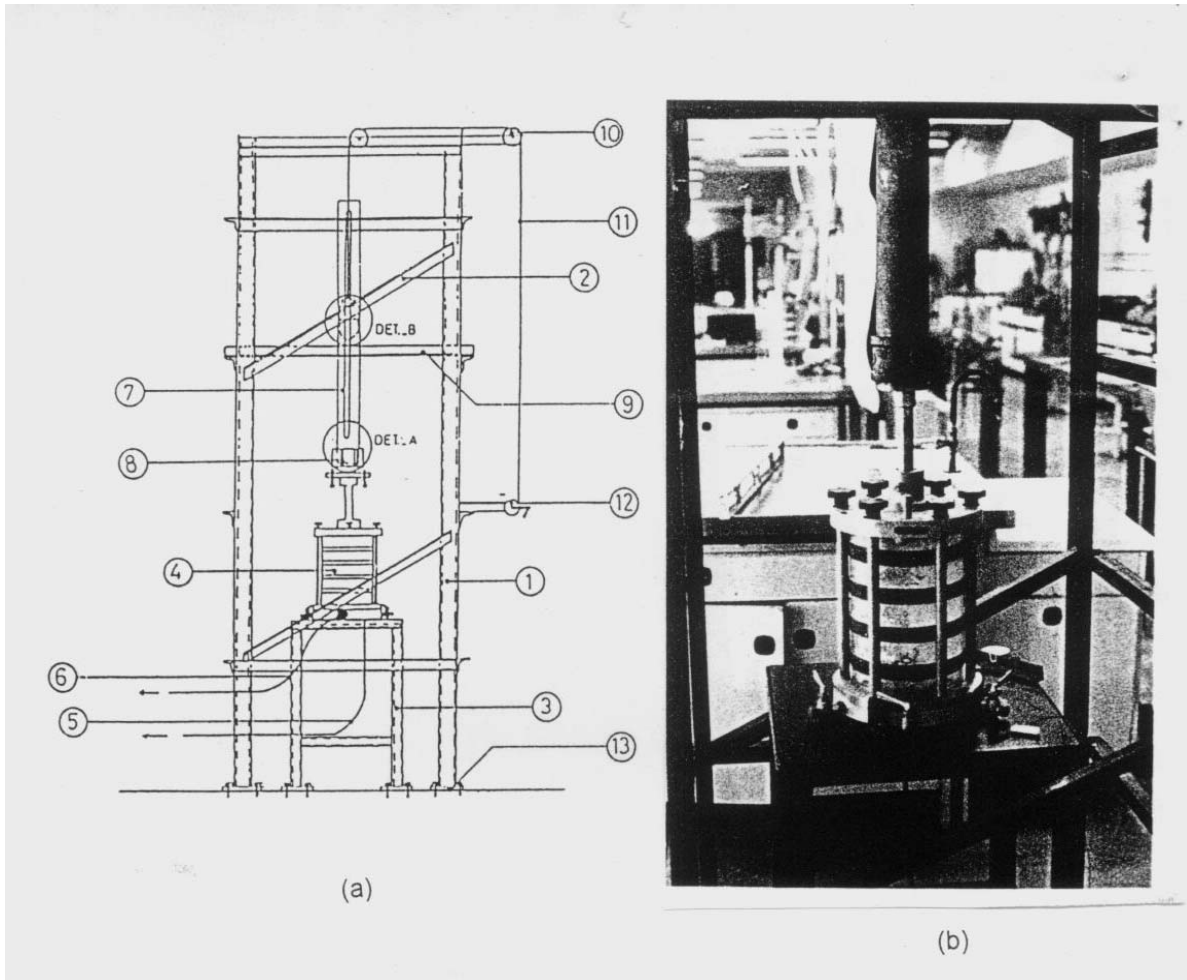


Fig. (5) -. Dynamic testing apparatus.
(a) Schematic diagram. (b) Photograph.

- | | |
|--|--|
| 1. The frame of the device-4 channels 76x36x6 mm | 8. The hammer stopper – modified bushing |
| 2. Bracing 36x36x6 mm | 9. Angles holding the hammer's guide |
| 3. The table of the triaxial test | 10. Rollers for lifting the weight |
| 4. Modified triaxial cell | 11. Steel cable for lifting the weight |
| 5. Load cell cable to the electronic circuit | 12. A jack for lifting the weight to the desired position |
| 6. Displacement transducer cable to the electronic circuit | 13. Bearing plates to fix the frame and the cable to the ground 150x150x80 mm. |
| 7. The hammer's guide 90 mm steel pipe | |

6.6 Method of Testing:

Sand samples were tested by Baho (1989) and Farhan (1989) at both loose and dense states, i.e. at initial relative densities approximately equal to 25 % and 75 %, respectively.

The triaxial cell was assembled and the confining air was applied as required. The magnitudes of vacuum and confining pressures were read on separate Bourdon gauges. The falling mass was raised to heights of 20 cm, 35cm and 60 cm. Samples were tested at confining pressures of 30, 60, 100 and 200 kN/m² for each initial relative density. After the application of the confining pressure, the relative density changed due to compression caused by the equal all round pressure where the relative density increased as the confining pressure was increased.

Table 1 shows the pre-shear relative densities after the application of the confining pressure.

7. Analysis and Results:

The triaxial sample was modeled by 10 four-noded isoparametric serendipity type elements and the problem is considered to be axisymmetric. The mesh of the problem is shown in Figure (6).

Double Impact Problems:

The problem consists of three cases depending on the height of drop:

- A-1) D20, height of drop = 20 cm.
- A-2) D35, height of drop = 35 cm.
- A-3) D60, height of drop = 60 cm.

Figure (7) shows the stress - strain relationship for the case of cell pressure, $\sigma_3 = 30 \text{ kN/m}^2$ and initial relative density, $Dr = 50\%$ (after Baho, 1989). The properties of the material required for the analysis are summarized in Table (2).

Table (1) - Pre-shear relative densities, (after Baho,1989).

Relative Density (%)	Confining Pressure kN/m^2			
	30.0	60.0	100.0	200.0
75.0	77.8	80.0	82.0	
50.0	52.0	55.70	58.0	
25.0	28.6	32.2	-	

Table (2) - Material Properties.

Material property	Value
Pre-shear relative density, D_r	50 %
Initial modulus of elasticity, E_i	74 MN/m^2
Poisson's ratio, ν	0.30 (assumed)
Initial bulk modulus, K_i	61.67 MN/m^2
Initial shear modulus, G_i	28.46 MN/m^2
Porosity, n	0.452
Bulk density, ρ	1450 kg/m^3

The damping ratios were calculated from the results of Farhan (1989). They were 0.843, 0.873 and 0.867 for heights of drop of 20, 35 and 60 cm, respectively.

In this problem, the material used is dry, i.e., the terms concerning the pore fluid are neglected, and this was done by considering the sample fully drained through choosing the appropriate boundary conditions. The time step was taken as (0.05) sec. Figure (8) shows the kinematic yield surfaces in p_i plane for the initial state at middle of the sample (element 5). A series of tests was made by Baho (1989) and Farhan (1989) by applying a double impact load on sand samples. Figure (9) shows the stress-strain relationships for the two impact series for the case of confining pressure $\sigma_3 = 30 \text{ kN/m}^2$ and initial relative density, $Dr = 75\%$. The ALTERNAT model parameters were calculated by the procedure developed by Fattah (1999) and are listed in Table (3).

Table (3) - ALTERNAT model parameters for the problem.

Parameter	Value
Pa	105 kN/m^2
V	0.12
A	0.001
AP	0.401
E	1.892
EP	0.313
LB	0.30
EE	1.27
EEP	0.203
Ni	0.452
Nd	0.367
K	1.0
GK	0.461

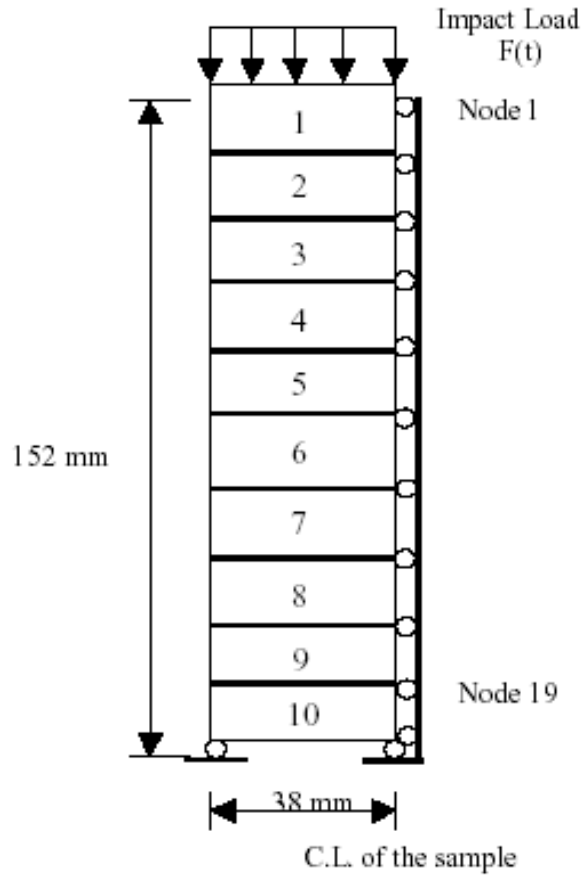


Fig. (6) - The finite element mesh.

Figure (10) shows a comparison between the measured and predicted forces at the top of the sample. The comparison between the measured and predicted displacements is shown in Figure (11).

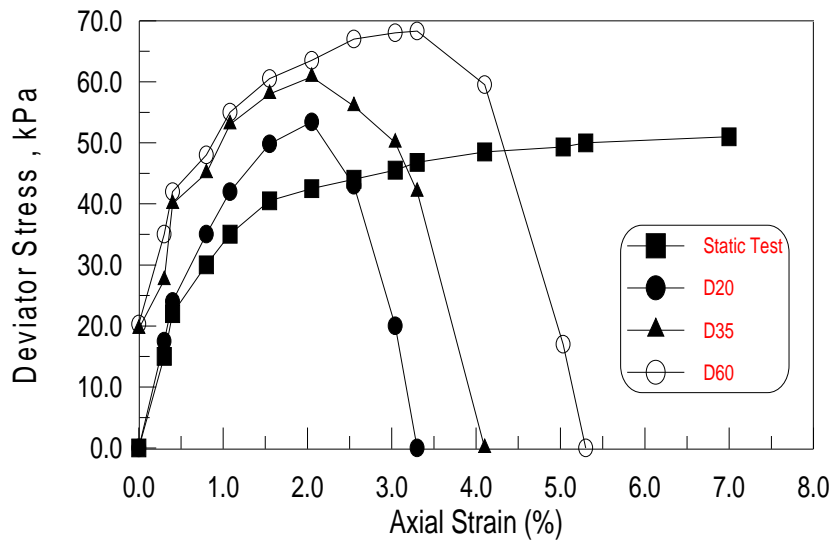


Fig. (7) - Stress – strain relationship for $\sigma_3 = 30 \text{ kN/m}^2$, $D_r = 50\%$ (after Baho, 1989).

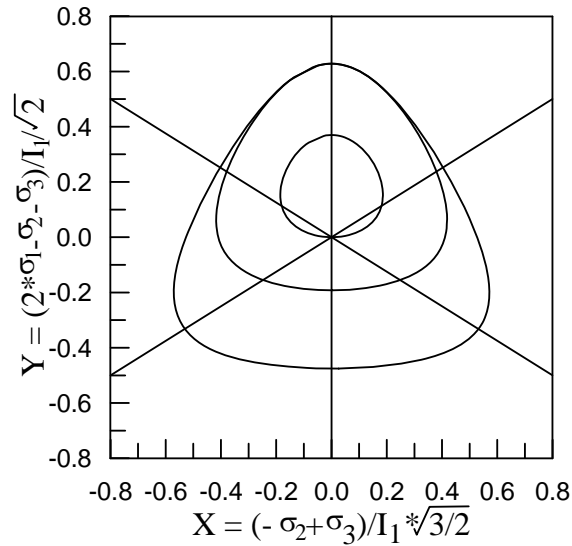


Fig. (8) - Kinematic yield surfaces in pi plane (initial state) for element 5.

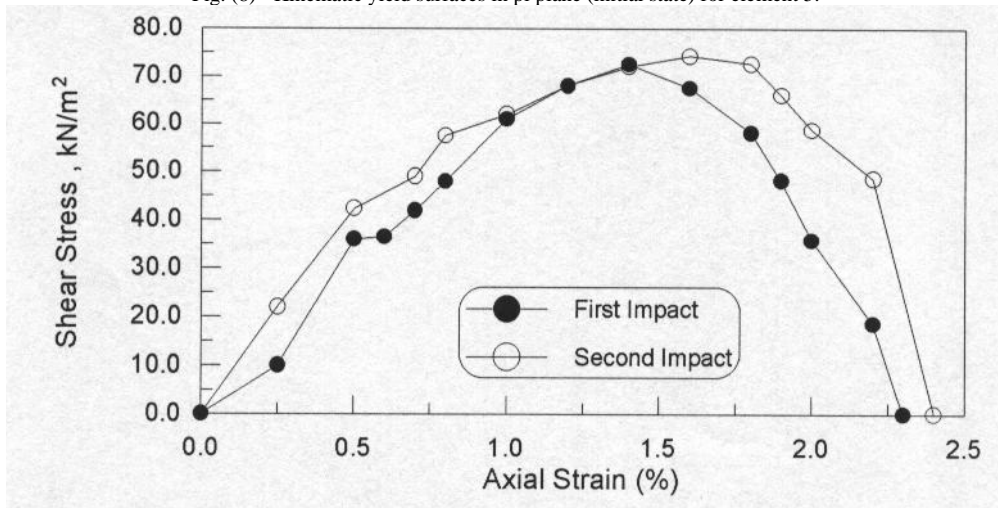
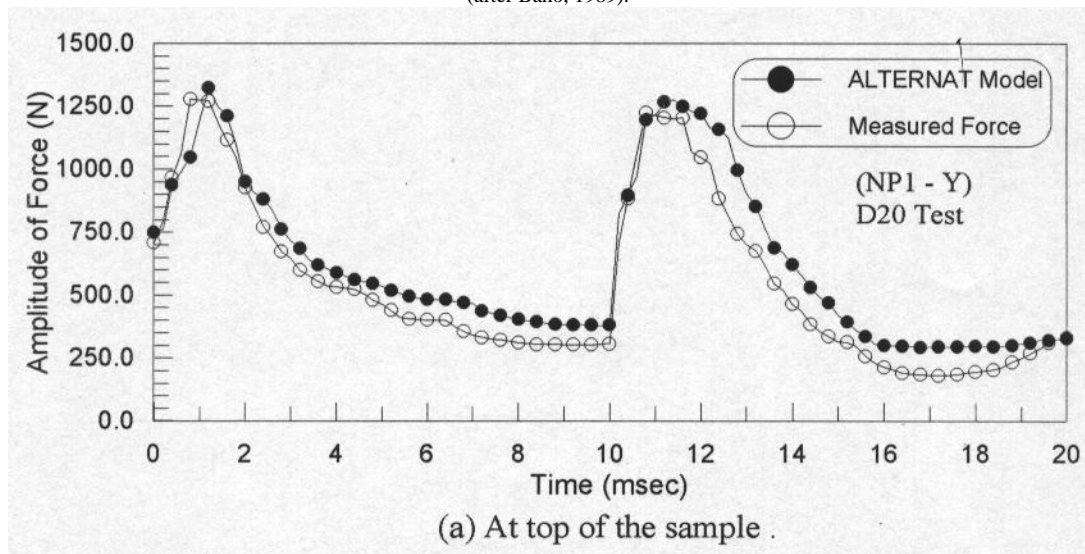


Fig. (9) – Stress-strain relationships for the two-impact series $\sigma_3 = 30 \text{ kN/m}^2$, $D_r = 50\%$, (after Baho, 1989).



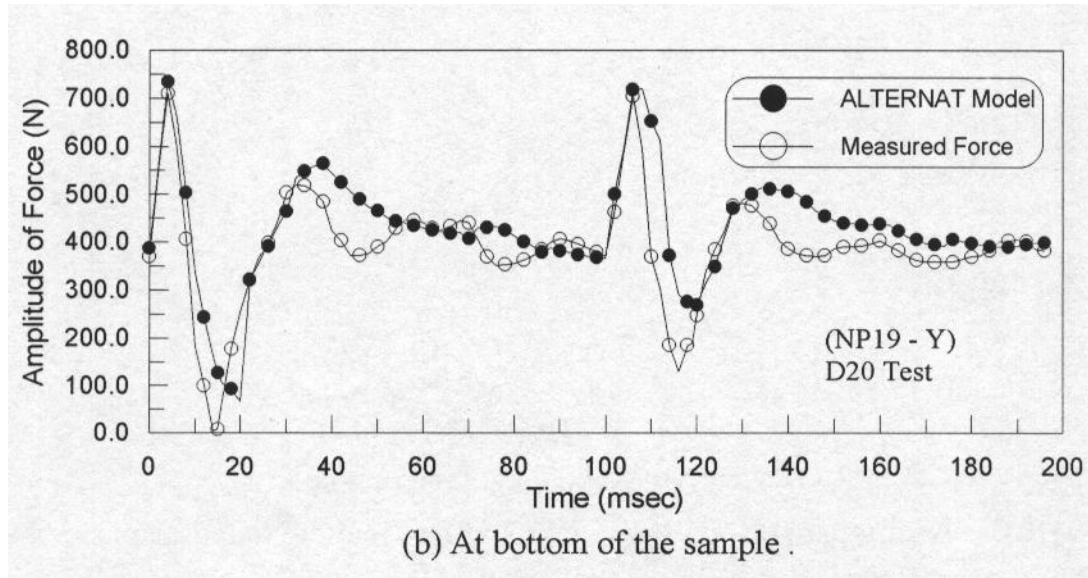
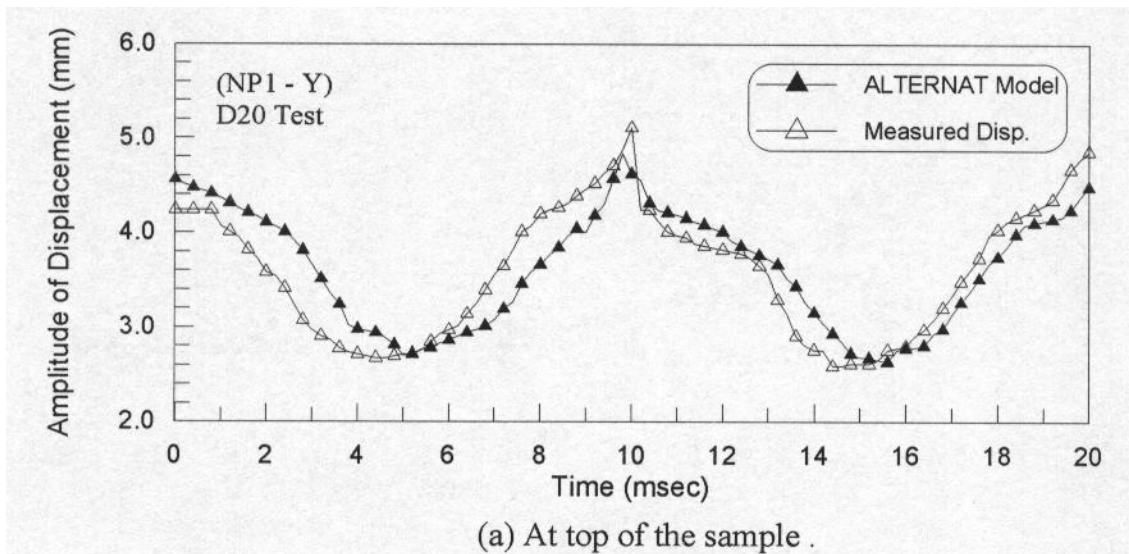


Fig. (10) – A comparison between the measured and predicted forces at top and bottom of the sample subjected to two impacts using the ALTERNAT model for $\sigma_3 = 30 \text{ kN/m}^2$, $Dr = 75\%$, height of drop = 20 cm.

It is concluded that the ALTERNAT model gives very good predictions for dense ($Dr = 75\%$) sands when subjected to double impacts. The small differences between the results and the experimental values may be attributed to the approximations used for some parameters required by the ALTERNAT model. In spite of these differences, the dynamic response is acceptable.



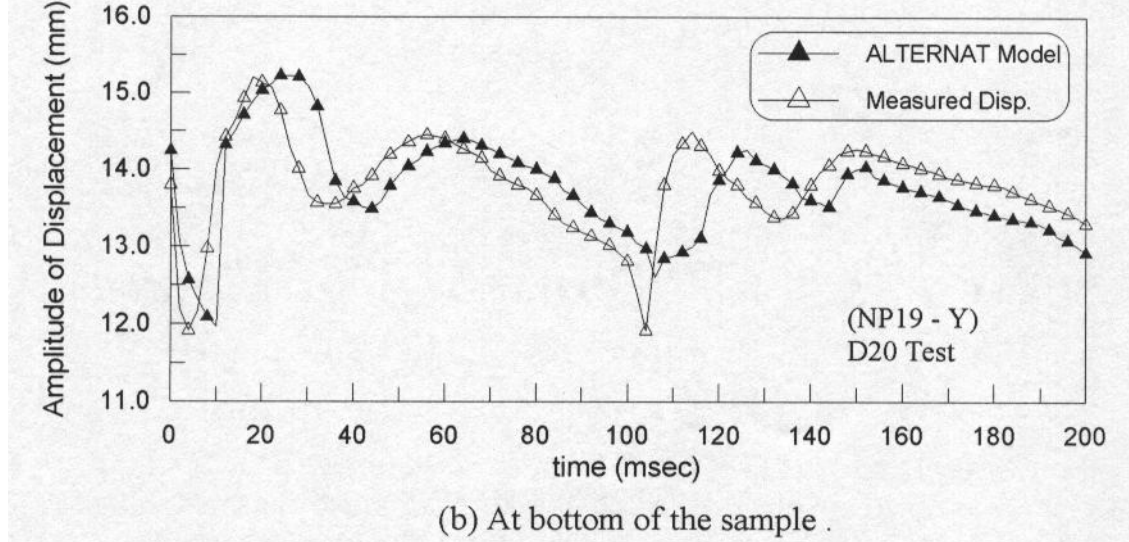


Fig. (11) – A comparison between the measured and predicted displacements at top and bottom of the sample subjected to two impacts using the ALTERNAT model for $\sigma_3 = 30$ kN/m², $D_r = 75\%$, height of drop = 20 cm.

Conclusions:

A general mixed finite element formulation (u-w- π) is presented in this paper. This formulation included the fluid inertia effects and the material response is considered compressible. The general formulation is applied in case of impact tests on dry sand samples made at the Civil Engineering Department, University of Baghdad (1989). The proper boundary conditions are selected in order to neglect the pore fluid forces and pore water pressure.

The double hardening model for alternating loading named ALTERNAT is used as a constitutive relation. The model parameters were determined analytically by applying the stress path required for the special triaxial tests to a theoretical model, namely, the endochronic model. The program LIQUEFAC modified by the authors gave good predictions for impact problems.

The ALTERNAT model gives very good predictions for dense ($D_r = 75\%$) sands when subjected to double impacts. The small differences between the results and the experimental values may be attributed to the approximations used for some parameters required either to the endochronic model or the ALTERNAT model. In spite of these differences, the dynamic response is acceptable.

References:

- [1] Awad, A. A. A., (1990), (A Numerical Model for Blast- Induced Liquefaction Using Displacements-Pore Pressure Formulations), Ph.D. thesis, Colorado State University.
- [2] Baho, N. K., (1989), (Experimental Investigation of Impact and Static Strength of Rutba Sand), M.Sc thesis, University of Baghdad.
- [3] Bazant, Z. P. and Krizek, R. J., (1976), (Endochronic Constitutive Law for Liquefaction of Sand), Journal of Engineering Mechanics, ASCE, Vol. 102, EM2, p. p. 225 - 238.
- [4] Biot, M. A., (1962), (Mechanics of Deformation and Acoustic Propagation in Porous Media), Journal of Applied Physics, 33, pp. 1482 -1498.
- [5] Farhan, S. S., (1989), (Damping Characteristics of an Iraqi Sand), M.Sc. thesis, University of Baghdad.
- [6] Fattah, M. Y., (1999), (The Non-Linear Dynamic Behaviour of Soils), Ph.D. dissertation, University of Baghdad.
- [7] Lade, P. V. and Duncan, J. M., (1975), (Elasto-Plastic Stress - Strain Theory for Cohesionless Soil), Journal of Geotechnical Engineering Division, ASCE, Vol. 101, GT10, pp. 1037 - 1053.
- [8] Mei, C. C. and Foda, M. A., (1982), (Boundary Layer Theory of Waves in a Poro-Elastic Sea Bed), Chapter 2 in "Soil Mechanics-Transient and Cyclic Loads", edited by G. N. Pande and O. C. Zienkiewicz, pp. 17 - 35.
- [9] Lewis, R. W. and Schrefler, B. A., (1998), (The Finite Element Method in the Static and Dynamic Deformation and Consolidation of Porous Media), second edition, John Wiley & Sons, Inc., USA.
- [10] Molenkamp, F., (1980), (Elasto-Plastic Double Hardening Model, MONOT), Report, Delft Geotechnics.
- [11] Molenkamp, F., (1987), (Kinematic Model for Alternating Loading, ALTERNAT), Report, Delft Geotechnics.
- [12] Molenkamp, F., (1990), (Reformulation of ALTERNAT Model to Minimize Numerical Drift Due to Cyclic Loading), Report, University of Manchester.
- [13] Namiq, L. I., Farhan, S. S., and Baho, N. K., (1990), (A Transient Load Triaxial Testing Device for Soils), Ministry of Planning, Central Organization for Measurement and Quality Control, Department of Industrial Royalty, Section of Invention Patencies and Industrial Models, Patency No. 2294, Baghdad, Iraq.
- [14] Simon, B.R., Wu, J. S. S., Zienkiewicz, O. C. and Paul, D. K., (1986), (Evaluation of u-w and u- π Finite Element Methods for the Dynamic Response of Saturated Porous Media Using One-Dimensional Models), International Journal for Numerical and Analytical Methods in Geomechanics, Vol. 10, pp. 461-482.
- [15] Zienkiewicz, O.C., (1977). (The Finite Element Method), McGraw-Hill Book Company.

- [16] Zienkiewicz, O. C., and Bettess, P., (1982), (Soils and Other Saturated Media Under Transient, Dynamic Conditions, General Formulation and the Validity of Various Simplifying Assumptions). Chapter 1 in "Soil Mechanics - Transient and Cyclic Loads", Edited by G.N. Pande and O.C. Zienkiewicz.
- [17] Zienkiewicz, O. C., Leung, K. H., Hinton, E. and Chang, C. T., (1982), (Liquefaction and Permanent Deformation Under Dynamic Conditions-Numerical Solution and Constitutive Relations), Chapter 5 in "Soil Mechanics-Transient and Cyclic Loads", edited by G. N. Pande and O. C. Zienkiewicz, pp. 71 – 103.
- [18] Zienkiewicz, O. C. and Taylor, R. L., (2000), (The Finite Element Method), Volume 1, "The Basis", fifth edition, Butterworth-Heinemann.